Long non-coding RNA *DINO* promotes cisplatin sensitivity in lung adenocarcinoma via the p53-Bax axis

Zhile Liu[1#], Qi Wang[2#], Yue Bi[3#], Alexey S. Chubarov[4], Ying Li[1], Lu Liu[1], Xia Yang[1], Elena V. Dmitrienko[4], Yanfang Zheng[1]

[1]Department of Medical Oncology, Affiliated Cancer Hospital & Institute of Guangzhou Medical University, Guangzhou, China; [2]Department of Radiotherapy, Nanyang Central Hospital, Nanyang, China; [3]Department of Radiation Oncology, the First Affiliated Hospital of Sun Yat-sen University, Guangzhou, China; [4]Institute of Chemical Biology and Fundamental Medicine, Siberian Branch of the Russian Academy of Sciences, Novosibirsk, Russia

Contributions: (I) Conception and design: Y Zheng, EV Dmitrienko, Z Liu; (II) Administrative support: Y Zheng, EV Dmitrienko; (III) Provision of study materials or patients: Q Wang, Y Bi; (IV) Collection and assembly of data: AS Chubarov, Y Li; (V) Data analysis and interpretation: Z Liu, L Liu, X Yang; (VI) Manuscript writing: All authors; (VII) Final approval of manuscript: All authors.

[#]These authors contributed equally to this work.

Correspondence to: Yanfang Zheng, MD, PhD. Department of Medical Oncology, Affiliated Cancer Hospital & Institute of Guangzhou Medical University, No. 78, Hengzhigang Road, Guangzhou 510095, China. Email: zheng2020@gzhmu.edu.cn; Elena V. Dmitrienko, PhD. Institute of Chemical Biology and Fundamental Medicine, Siberian Branch of the Russian Academy of Sciences, 8 Lavrentyev Ave, Novosibirsk 630090, Russia. Email: elenad@niboch.nsc.ru.

Background: The damage-induced non-coding (*DINO*) RNA is a newly identified long non-coding RNA (lncRNA) found in human cells with DNA damage. The treatment of tumors with cisplatin can induce DNA damage; however, whether the lncRNA *DINO* is involved in the treatment of non-small cell lung cancer (NSCLC) has not yet been elucidated.

Methods: The expression of the lncRNA *DINO* in lung adenocarcinoma cells was detected using quantitative real-time polymerase chain reaction (qRT-PCR). The lung adenocarcinoma cell line, A549, and derived cisplatin-resistant cell line, A549R, were selected to construct cell models with lncRNA *DINO* overexpression or interference via lentiviral transfection. After cisplatin treatment, changes in the apoptosis rate were measured. Changes in the *p53-Bax* axis were detected by qRT-PCR and Western blot. Cycloheximide (CHX) interference demonstrated the stability of *p53* with new protein production induced by the lncRNA *DINO*. The *in vivo* experiments involved intraperitoneal injection of nude mice with cisplatin after subcutaneous tumor formation, and the tumor diameters and weights were recorded. Immunohistochemistry and hematoxylin and eosin (H&E) staining were performed following tumor removal.

Results: We found that the lncRNA *DINO* was significantly down-regulated in NSCLC. *DINO* overexpression enhanced the sensitivity of NSCLC cells to cisplatin, while *DINO* down-regulation decreased the sensitivity of NSCLC cells to cisplatin. Mechanistic investigation indicated that *DINO* enhanced the stability of *p53* and mediated the activation of the *p53-Bax* signaling axis. Our results also demonstrated that the lncRNA *DINO* could partially reverse cisplatin resistance induced by silencing the *p53-Bax* axis, and could inhibit subcutaneous tumorigenesis in nude mice after cisplatin treatment *in vivo*.

Conclusions: The lncRNA *DINO* regulates the sensitivity of lung adenocarcinoma to cisplatin by stabilizing *p53* and activating the *p53-Bax* axis, and thus, may be a novel therapeutic target to overcome cisplatin resistance.

Keywords: Lung adenocarcinoma (LUAD); long noncoding RNA *DINO*; *p53*; cisplatin resistance

Introduction

According to the 2023 cancer statistics, lung cancer is the leading cause of cancer-related death, with 350 people dying of lung cancer every day (1). Approximately 85% of lung cancer cases are non-small cell lung cancer (NSCLC), and lung adenocarcinoma (LUAD) is the most common subtype of NSCLC (2). Patients with NSCLC can be treated with chemotherapy, surgery, radiation, targeted therapy, or immunotherapy to improve survival (3). However, due to the lack of typical clinical symptoms for early-stage lung cancer, 65–80% of patients are diagnosed with middle- or advanced-stage disease (4). Chemotherapy is still the primary treatment option for patients without a driver gene mutation or with recurrent lung cancer (5). Platinum compounds have a broad antitumor spectrum, and their mechanism involves forming a complex with DNA via cross-linking to hinder the processes of cell division and replication, thereby exerting an anticancer effect (6,7). Despite the emergence of new-generation platinum drugs, the side effects of high-dose cisplatin (DDP) therapy and drug resistance still limit efficacy (8,9). Therefore, there is an urgent need to develop novel strategies to enhance the therapeutic effect of platinum drugs.

Long non-coding RNA (lncRNA) is a type of long (>200 nucleotides) non-coding RNA molecule that does not have the typical function of encoding a protein (10). Recent research has shown that lncRNAs are involved in the occurrence of cancer pathological conditions, a component of the tumor microenvironment, and the modification of chemoresistance (11-15). In November 2016, Schmitt *et al.* discovered that human cells transcribed a new lncRNA after being treated with doxorubicin and named lncRNA *DINO* (damage-induced non-coding) (16). Upregulation of the lncRNA *DINO* stabilizes the *p53* protein and activates the DNA damage repair pathway (17). The treatment of tumors with DDP can also cause DNA damage; however, whether the lncRNA *DINO* is involved in the treatment of LUAD remains unclear.

The tumor suppressor *p53* is critically involved in DDP-induced apoptosis (18-20). After DNA damage, DNA repair requires *p53* to activate *p21*, which blocks the G2/M phase (21). However, if the DNA damage is too severe to repair, the upregulation of *Bax* by *p53* promotes the apoptotic process via the mitochondrial pathway (22,23). Therefore, when *p53* is involved in the treatment of NSCLC with DDP, it is necessary to pay attention to the downstream targets of *p53* to find suitable therapeutic targets.

In this study, we hypothesized that the lncRNA *DINO* affects DDP resistance via the *p53-Bax* axis through *p53* stability. To verify this hypothesis, we detected the expression level of the lncRNA *DINO* in NSCLC cell lines. Through *in vitro* and *in vivo* experimental assays, we further investigated the functional relevance of the lncRNA *DINO* in NSCLC chemoresistance. We present the following article in accordance with the ARRIVE reporting checklist (available at https://jtd.amegroups.com/article/view/10.21037/jtd-23-465/rc).

Methods

Materials and reagents

Phosphate-buffered saline (PBS), RPMI-1640 medium, and fetal bovine serum (FBS) were procured from Gibco (Grand Island, USA). Cell Counting Kit-8 (CCK-8) and cycloheximide (CHX) were obtained from GLPBIO (California, USA). PEN-STREP solution (10,000 units/mL penicillin and 10 mg/mL streptomycin) was produced by Biological Industries (Beit Haemek, Israel). An Annexin V-fluorescein isothiocyanate (FITC)/propidium iodide (PI) cell apoptosis detection kit was provided by KeyGEN Biotech (Nanjing, China). DDP (#D8810) was purchased from Solarbio (Beijing, China). Antibodies against the following proteins were used: *p53* (Proteintech, China), *p21* (Proteintech, China), *Bax* (CST, USA), poly ADP-ribose polymerase (*PARP*) (Wanleibio, China), and glyceraldehyde 3-phosphate dehydrogenase (*GAPDH*) (Bioworld Technology, China).

Highlight box

Key findings
- The lncRNA *DINO* stabilizes *p53* and activates the *p53-Bax* axis, thereby regulating the sensitivity of lung adenocarcinoma to cisplatin.

What is known and what is new?
- (I) DNA damage induces the expression of the lncRNA *DINO*; (II) the lncRNA *DINO* stabilizes wild-type *p53*;
- (I) Cisplatin treatment of lung cancer stimulates lncRNA *DINO* expression; (II) the lncRNA *DINO* activates the p53-Bax axis to enhance cisplatin sensitivity.

What is the implication, and what should change now?
- The lncRNA *DINO* may be a novel therapeutic target to overcome cisplatin resistance.

Cells and cell culture

The human lung carcinoma cell lines, H460, A549, H1299, H1993, Hcc827, PC9, and H1975, and the normal lung epithelial cell line HBE were obtained from American Type Culture Collection (ATCC, VA, USA). The DDP-resistant cell line, A549R, was established from A549 cells in our laboratory by culturing A549 cells with increasing concentrations of DDP for 6 months; A549R cells were cultured in a medium containing DDP at a concentration of 1 μg/mL to maintain resistance. All the human lung carcinoma cell lines were cultured in RPMI-1640 medium containing 10% heat-inactivated FBS and 1% PEN-STREP solution in an environment of 5% CO_2 at 37 ℃.

Vector construction and transduction

Cell transfection was performed using Lipofectamine 3000 Reagent (Invitrogen, USA) according to the manufacturer's protocol. *DINO* small interfering (si) RNAs (si-*DINO*-1 and si-*DINO*-2) or a *p53* interference plasmid were synthesized by Suzhou GenePharma Co., Ltd. (China). A lentiCRISPRv2 interference plasmid for the *Bax* gene was obtained from Guangzhou IGE Biotechnology Co., Ltd. (China). A specific interference sequence (si-*DINO*-2) was cloned into the pLKO.1-puro plasmid and cotransfected with the pVSV-G, pMDLg, and pRSV-Rev plasmids into HEK293T cells to generate viruses. A lentivirus (LV) encoding the lncRNA *DINO* gene was purchased from Shanghai Genechem Co., Ltd. (China). Information on the interference sequences is shown in Table S1.

RNA isolation and quantitative real-time polymerase chain reaction (qRT-PCR)

All steps were performed in accordance with the manufacturer's instructions. Total RNA was extracted using TRIzol (Takara, Japan), and the RNA concentration was detected with a NanoDrop2000 spectrophotometer (Thermo Fisher, USA).

Complementary DNA (cDNA) was synthesized by reverse transcription of RNA by using a PrimeScript RT reagent kit (Takara). qRT-PCR was performed using SYBR premix (Takara) and a CFX96 PCR detection system (Bio-Rad, USA). GAPDH was used as a standardization control, and the results were calculated by the $2^{-\Delta\Delta Ct}$ method. The primer sequence information is shown in Table S2.

CCK-8 assay

A total of 10,000 cells per well were cultured in 96-well plates and incubated at 37 ℃ overnight. The next day, the cells were treated with various concentrations of DDP for 48 h and then incubated with 10 μL of CCK-8 solution added to each well (100 μL of medium). After incubation at 37 ℃ for 1 h, the absorbance at 450 nm optical density (OD) value was detected using a microplate reader (Biotex, USA). Moreover, the half-maximal inhibitory concentration (IC50) values were then calculated from the OD value using SPSS software (Chicago, IL, USA). Each experiment was performed in triplicate.

Cell apoptosis analysis

The analysis of NSCLC cell apoptosis was performed using an Annexin V-FITC/PI cell apoptosis detection kit. Briefly, all cells were harvested using trypsin without ethylene diamine tetraacetic acid (EDTA) and washed twice with ice-cold PBS. Next, the cells were resuspended in 1× binding buffer at 1×10^6 cells/mL. Five microliters of PI and 5 μL of Annexin V-FITC were added, and the suspension was incubated for 15 min at room temperature protected from light and then analyzed using a CytoFLEX cytometer (Beckman-Coulter, USA). Finally, the analysis results were analyzed using FlowJo software (version 10.6.0, LLC, Oregon, USA).

Western blotting

After processing the cells according to the experimental requirements, the samples were washed twice with ice-cold PBS and lysed with Radio Immunoprecipitation Assay (RIPA) buffer. Next, after centrifugation at 12,000 rpm for 15 min, the samples were boiled in a sodium dodecyl sulfate (SDS) loading buffer and separated on 10% SDS-polyacrylamide gel electrophoresis (SDS-PAGE). The proteins were transferred to polyvinylidene fluoride (PVDF) membranes, which were blocked with 5% bovine serum albumin (BSA) for 2 h at 30 ℃, and then incubated with primary antibodies at 4 ℃ overnight. Next, the membranes were incubated for 2 h at 30 ℃ with horseradish peroxidase (HRP)-conjugated secondary antibodies. Using enhanced chemiluminescence (ECL) detection reagents (Millipore, USA), the membranes were visualized with a ChemiDoc

XRS+ system (Bio-Rad, USA).

CHX chase assay

Stable cell lines were constructed with a lentiviral system, and then the medium was supplemented with 25 µg/mL CHX (GLPBIO). After processing cells at the indicated times according to experimental need, the cells were washed with ice-cold PBS and collected in Eppendorf (EP) tubes, followed by the addition of lysis buffer containing protease inhibitors. Western blotting was performed as described previously to detect the levels of the *p53* protein.

Tumor xenograft experiments

According to the institutional guidelines of the Guangdong Province, 4- to 6-week-old female nude BALB/c mice were purchased from the Experimental Animal Center of Southern Medical University (Guangzhou, China). The nude mice were reared at 25 ℃ under a 12-h light/dark cycle in cages with sufficient space for exploration and access to fresh food and water at all times. According to the protocols outlined in the literature (24,25), a total of 10 nude mice were injected in the right flank with 200 µL of PBS containing 1×10^6 *DINO* overexpression LV vector-transfected A549R cells for xenograft tumor formation. Additionally, another 10 nude mice were injected with the same number of negative control (NC) LV vector-transfected A549R cells.

All mice were observed for 7 days; when the tumor volume reached 100 mm³, the 10 tumor-bearing nude mice overexpressing *DINO* were randomly divided into two groups (n=5 per group). The first group was injected intraperitoneally with DDP (2 mg/kg) every other day, while the second group was injected intraperitoneally with the same amount of PBS every other day. Similarly, 10 tumor-bearing NC gene nude mice were also randomly divided into two groups (n=5 per group). The first group was injected intraperitoneally with DDP (2 mg/kg) every other day, while the second group was injected intraperitoneally with the same amount of PBS every other day. During the treatment, the long and short diameters of the tumors were recorded every 3 days. When the length and diameter of the tumors in the nude mice reached approximately 1 cm, all of the mice were euthanized by CO_2 suffocation, after which the tumor was removed, weighed, and photographed. The study was started in Southern Medical University. Animal experiments were performed under a project license (No. 2018A0303130233) granted by institutional ethics board of Southern Medical University, in compliance with institutional guidelines for the care and use of animals. A protocol was prepared before the study without registration.

Immunohistochemistry (IHC) and hematoxylin and eosin (H&E) staining

IHC staining was performed as follows: first, subcutaneous tumors from the nude mice were fixed in formalin, embedded in paraffin, and cut into 5-µm-thick sections. After deparaffinization and rehydration with xylene and ethanol, the sections were boiled with citrate for antigen retrieval and treated with hydrogen peroxide (3%) to abrogate the endogenous peroxidase activity. Next, the non-specific staining was blocked with BSA, and the sections were incubated with a primary antibody overnight at 4 ℃. Subsequently, secondary antibodies (Dako, Denmark) coupled to HRP were applied, and detection was performed with 3,3-diaminobenzidine (DAB) incubation, followed by hematoxylin counterstaining.

H&E staining was conducted as follows: after dewaxing and rehydration, the sections were stained with H&E. Finally, the sections were washed with pure water and observed under a microscope (Leica, Heidelberg, Germany).

Statistical analysis

Data are expressed as the mean ± standard deviation (SD) of at least three independent experiments. Statistical analysis was performed using the *t*-test or one-way analysis of variance (ANOVA). All comparisons for which the P value was <0.05 were considered statistically significant.

Results

LncRNA DINO was significantly down-regulated in NSCLC and increased by DDP

To investigate the potential role of the lncRNA *DINO* in NSCLC, we first used real-time PCR to explore the expression of the lncRNA *DINO*. The results showed that the gene expression levels of *DINO* were significantly down-regulated in the H460, A549, H1299, H1993, Hcc827, PC9, and H1975 cell lines compared with the normal lung epithelial cell line HBE (*Figure 1A*). To determine the role of the lncRNA *DINO* in mediating resistance to chemotherapy, the NSCLC cell line, A549, and DDP-resistant cell line,
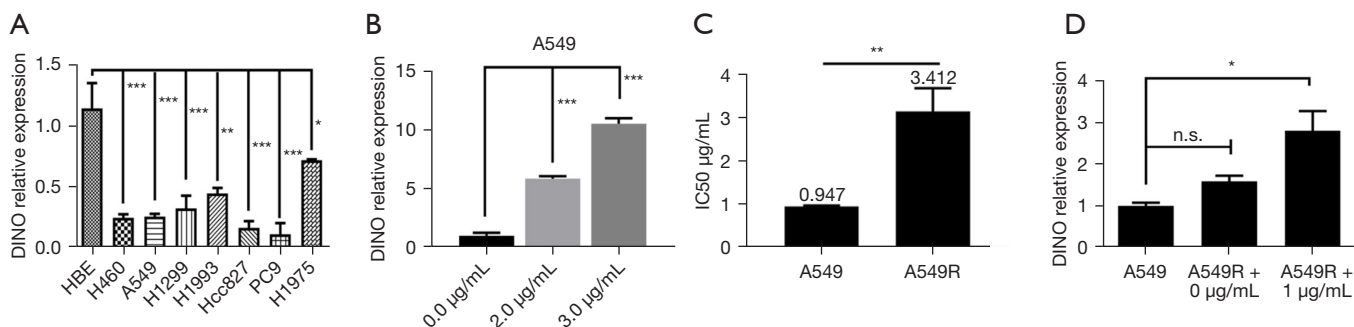
Figure 1 Cisplatin stimulates the expression of lncRNA *DINO*, which is downregulated in NSCLC cells. (A) Expression of lncRNA *DINO* in HBE, H460, A549, H1299, H1993, Hcc827, PC9, and H1975 cells. (B) Compared with the culture conditions of a normal drug-free medium, the lncRNA *DINO* of the A549 cell line was significantly increased by cisplatin in a dose-dependent manner. (C) The CCK-8 experiment was used to detect the IC50 value of A549 and A549R. (D) Compared with A549, there was no significant difference in the A549R-0 μg/mL group; however, lncRNA *DINO* was highly expressed in the A549R-1 μg/mL group. Three independent experiments were conducted. Error bars stand for the mean ± SD of at least three experiments. *, $P<0.05$; **, $P<0.01$; ***, $P<0.001$. CCK-8, Cell Counting Kit-8; DINO, damage-induced non-coding; lncRNA, long non-coding RNA; NSCLC, non-small cell lung cancer; SD, standard deviation; n.s., not significant.

A549R, were used to investigate the effect of DDP treatment. In the A549 cell line, we observed that the lncRNA *DINO* expression level was increased by DDP in a dose-dependent manner (*Figure 1B*). The CCK-8 assay showed that the IC50 of A549R cells was 3.412 μg/mL, which was ~3-fold higher than that of A549 cells (0.947 μg/mL) (*Figure 1C*). The lncRNA *DINO* was also highly expressed in the DDP-resistant cell line A549R, which was cultured in a medium containing DDP at a concentration of 1 μg/mL to maintain resistance. However, there were no significant differences between A549 and A549R cells cultured without DDP for 2 weeks (*Figure 1D*). These results suggested that the expression of the lncRNA *DINO* increased with DDP treatment in a dose-dependent manner in A549 and A549R cells; therefore, the lncRNA *DINO* might be involved in the DDP treatment of NSCLC cells.

LncRNA DINO enhanced the sensitivity of NSCLC cells to DDP

To determine the role of the lncRNA *DINO* in mediating sensitivity to chemotherapy, A549 and A549R cells were transfected with a control LV or *DINO* overexpression LV to upregulate the expression of the lncRNA *DINO* (*Figure 2A*). The CCK-8 assay showed that lncRNA *DINO* overexpression decreased the IC50 values of DDP in the A549 and A549R cell lines (*Figure 2B,2C*). Next, flow cytometry was performed to observe apoptosis; as

shown in *Figure 2D-2F)*, the cell apoptosis of A549 and A549R cells was markedly activated by overexpressing the lncRNA *DINO*.

Down-regulation of the lncRNA DINO decreased the sensitivity of NSCLC cells to DDP

The effect of lncRNA *DINO* down-regulation on DDP sensitivity was also investigated via the transfection of si-*DINO*-1 and si-*DINO*-2 on NSCLC cells. qRT-PCR confirmed that si-*DINO* significantly decreased the expression of the lncRNA *DINO* in the two cell lines after DDP treatment (*Figure 3A*). As shown in *Figure 3B-3D*, NSCLC cell apoptosis was found to be significantly suppressed after decreasing *DINO* expression by flow cytometry. The CCK-8 assay also showed that si-*DINO* increased the IC50 values of DDP in A549 and A549R cells (*Figure 3E-3H*).

### *LncRNA DINO targeted p53 in NSCLC regulation*

The knockdown achieved with siRNA-2 was better than that achieved with siRNA-1. Therefore, siRNA-2 was packaged into LVs to inhibit lncRNA *DINO* expression in NSCLC cells. Next, we investigated whether the lncRNA *DINO* regulates *p53* expression levels. By using qRT-PCR and Western blot assays, we found that the lncRNA *DINO* did not affect the transcription level of *p53* (*Figure 4A,4B*).
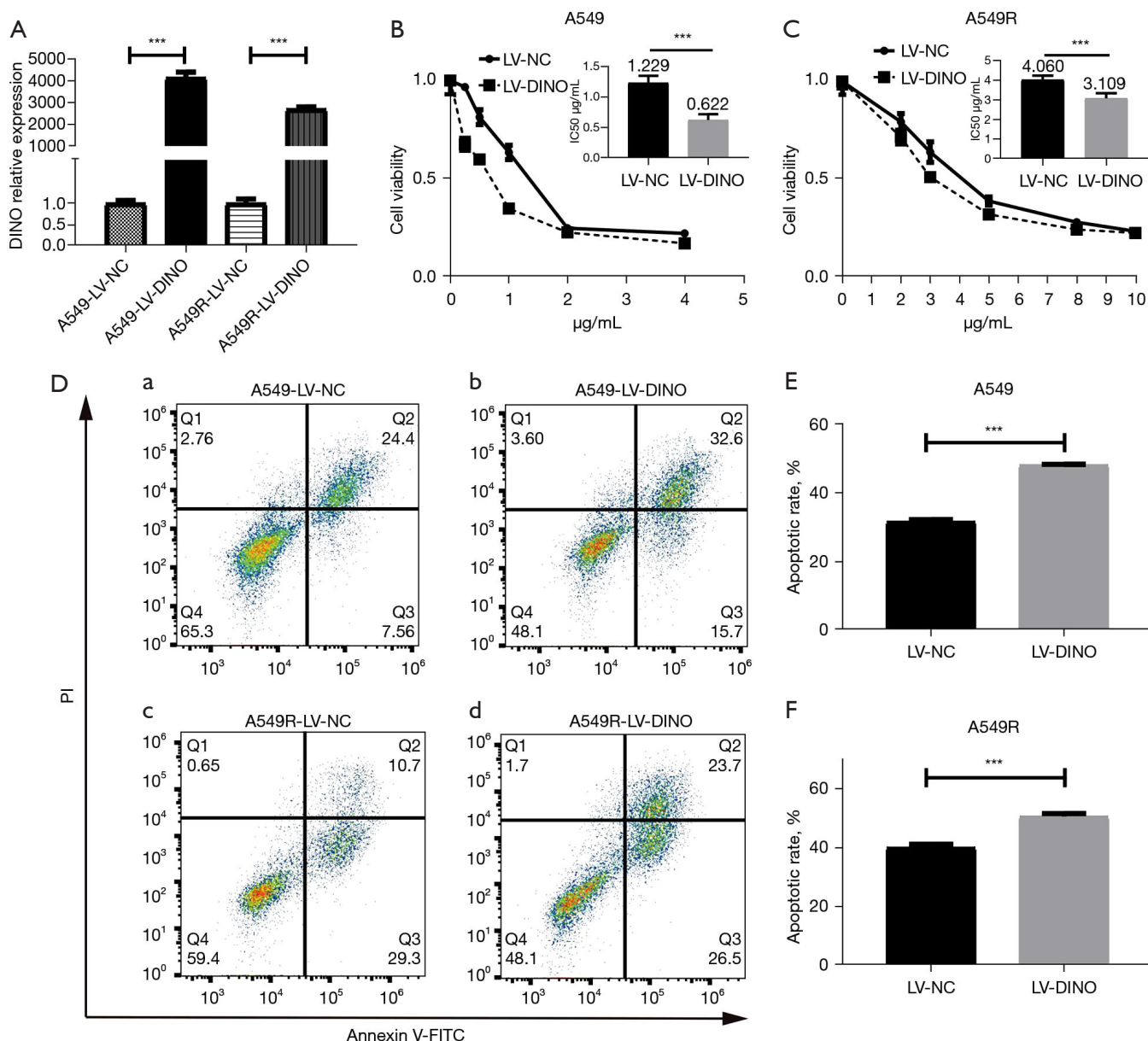
Figure 2 Upregulation of lncRNA *DINO* induces cell apoptosis in NSCLC cells. (A) LncRNA *DINO* was up-regulated more than 2,000 times in the A549-LV-*DINO* overexpression group and the A549R-LV-*DINO* group. (B,C) The cell viability of A549 and A549R cells after LV-NC or LV-*DINO* transfection was measured by CCK-8 assay. The IC50 of cisplatin was measured by three CCK-8 assays using SPSS 22.0. (D) The cell apoptosis rate in LV-NC or LV-*DINO* cells was determined by flow cytometry. (E) The statistical analysis of the total apoptosis rate in (D-a,b). (F) The statistical analysis of the total apoptosis rate in (D-c,d). Three independent experiments were conducted. Error bars stand for the mean ± SD of at least three experiments. ***, P<0.001. CCK-8, Cell Counting Kit-8; DINO, damage-induced non-coding; FITC, fluorescein isothiocyanate; lncRNA, long non-coding RNA; LV, lentivirus; NC, negative control; NSCLC, non-small cell lung cancer; SD, standard deviation.

However, in the Western blot assay, lncRNA *DINO* overexpression elevated the expression levels of *p53*, which were decreased by the down-regulation of lncRNA *DINO*

(*Figure 4C,4D*). CHX was used to block the synthesis of new *p53* protein. The results showed that after treatment with CHX for different durations, the expression of the *p53*

2204

Liu et al. LncRNA *DINO* enhances cisplatin sensitivity
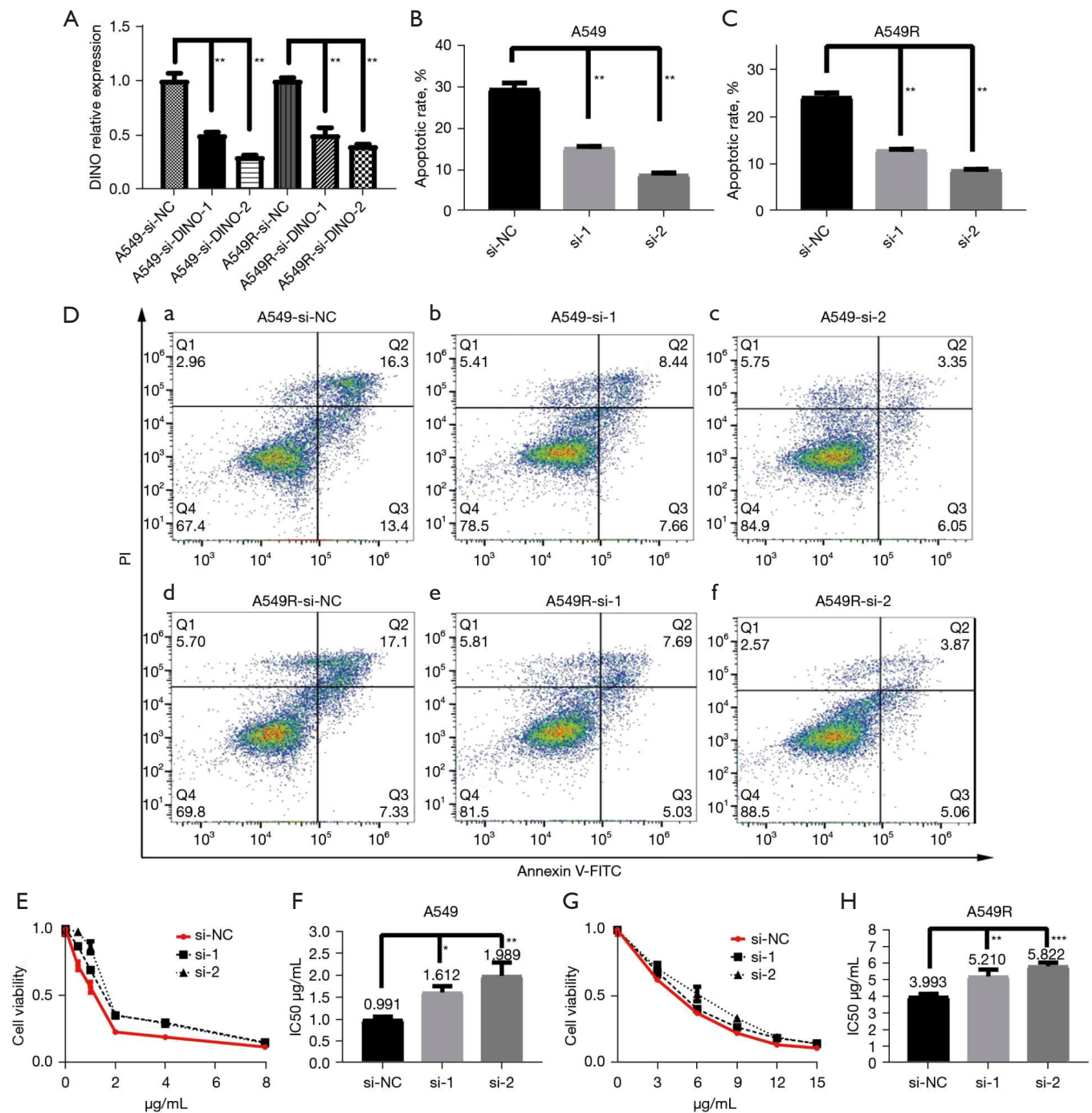
Figure 3 Downregulation of lncRNA *DINO* deduces cell apoptosis in NSCLC cells. (A) LncRNA *DINO* significantly reduces after transfection of siRNA. (B,C) The statistical analysis of the total apoptosis rate in (D). (D) The cell apoptosis rate in si-NC or si-*DINO* cells was determined by flow cytometry. (E,F) The viability of A549 cells after si-NC or si-*DINO* transfection was measured by CCK-8 assay. The IC50 of cisplatin was measured by tshree CCK-8 assays using SPSS 22.0. (G,H) The cell viability and IC50 of A549R cells. Three independent experiments were conducted. Error bars stand for the mean ± SD of at least three experiments. *, P<0.05; **, P<0.01; ***, P<0.001. CCK-8, Cell Counting Kit-8; DINO, damage-induced non-coding; FITC, fluorescein isothiocyanate; lncRNA, long non-coding RNA; NC, negative control; NSCLC, non-small cell lung cancer; PI, propidium iodide; SD, standard deviation; si, small interfering.
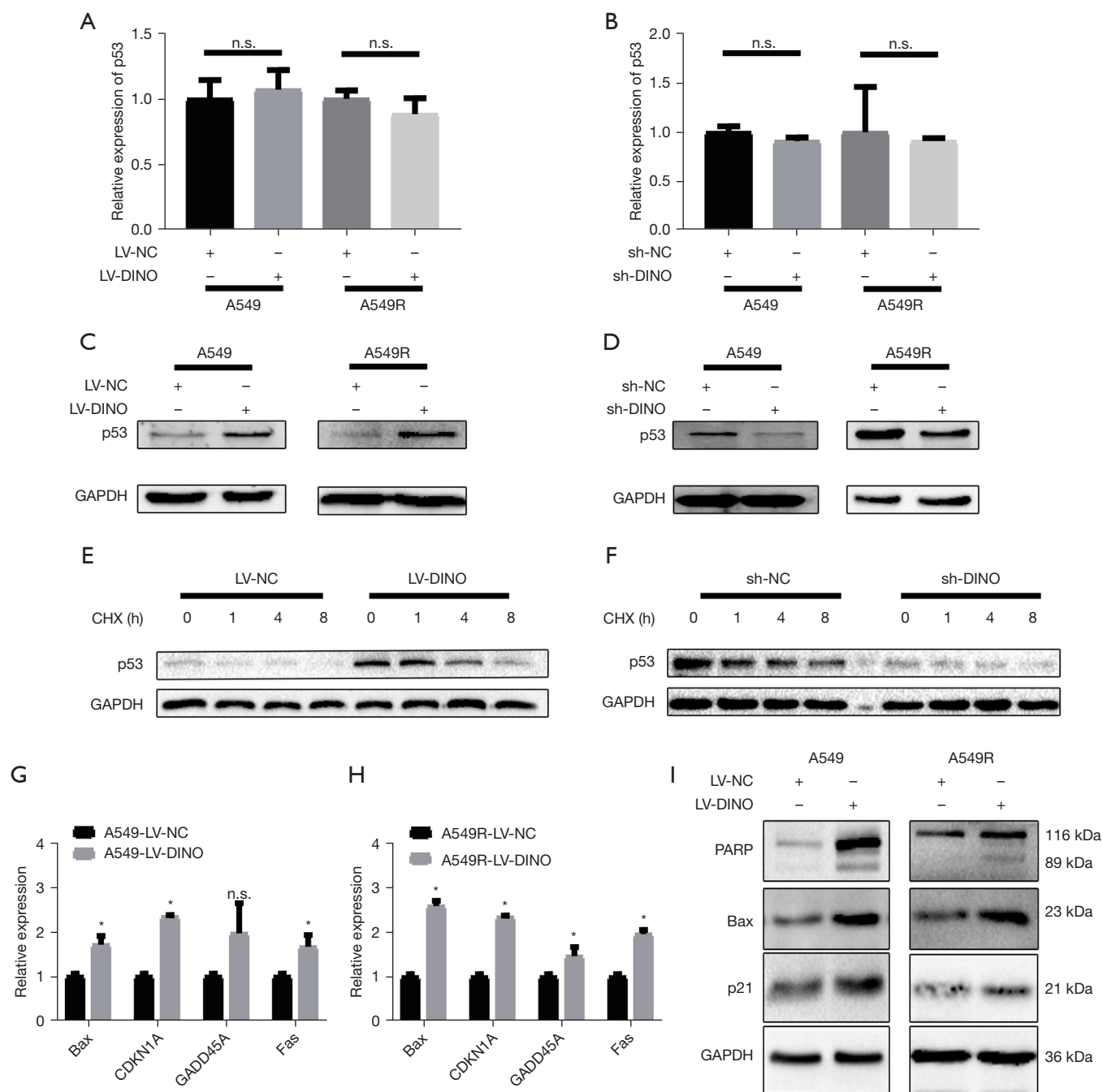
Figure 4 LncRNA *DINO* enhances the stability of *p53* and mediates the activation of the *p53-Bax* axis. (A,B) qRT-PCR was used to detect the mRNA expression level of *p53* in NSCLC cells transfected with the lncRNA *DINO* overexpression or interfering LV. (C,D) p53 protein levels in A549 and A549R cells transfected with the lncRNA *DINO* overexpression or interfering LV. (E,F) After treatment with CHX for the indicated times, Western blot analysis was performed to detect the p53 protein levels in A549 cells transfected with lncRNA *DINO* overexpression or interfering LV. (G,H) *p53*-target genes such as *Bax*, *CDKN1A*, *GADD45A*, and *Fas* were measured by qRT-PCR in NSCLC cells with upregulated lncRNA *DINO* expression. (I) PARP, Bax, and p21 were measured by Western blot in the NSCLC cells with upregulated lncRNA *DINO* expression. *, P<0.05. CHX, cycloheximide; DINO, damage-induced non-coding; lncRNA, long non-coding RNA; LV, lentivirus; NC, negative control; n.s., not significant; NSCLC, non-small cell lung cancer; PARP, poly-(ADP-ribose) polymerase; qRT-PCR, quantitative polymerase chain reaction; sh, small hairpin.

J Thorac Dis 2023;15(4):2198-2212 | https://dx.doi.org/10.21037/jtd-23-465

2206

Liu et al. LncRNA *DINO* enhances cisplatin sensitivity

protein in the LV-*DINO* group was higher than that in the NC group. At the same time, the expression of *p53* in the small hairpin (sh)-*DINO* group was lower (*Figure 4E,4F*).

The p53-Bax axis was involved in chemotherapy sensitivity induced by lncRNA DINO overexpression

Since the lncRNA *DINO* augments *p53* stability, we speculated that the lncRNA *DINO* activates the *p53* pathway. *qRT-PCR* showed that the *p53* downstream genes, *Bax*, *CDKN1A*, and *Fas*, were upregulated in two cell lines with stable overexpression of the lncRNA *DINO* (*Figure 4G,4H*). In the Western blot assay, the expressions of the proapoptotic proteins, *Bax* and cleaved *PARP*, were increased in the LV-*DINO* group (*Figure 4I*). These results suggested that the lncRNA *DINO* stabilizes *p53* and regulates the sensitivity of NSCLC cells to DDP, which may involve the *p53-Bax* axis.

Overexpression of DINO reversed the chemotherapy resistance induced by silencing the p53-Bax axis

We further examined whether the lncRNA *DINO* indeed exerts its function through the *p53-Bax* axis. First, an interference plasmid (sh-*p53*) targeting the *p53* mRNA transcript was synthesized and transfected into A549 cells. We co-transfected A549 cells with a lncRNA *DINO* overexpression LV and an interference plasmid (sh-*p53*), and the cells were divided into the following groups: *DINO*(–) + sh-*p53*(–), *DINO*(–) + sh-*p53*(+), *DINO*(+) + sh-*p53*(–), and *DINO*(+) + sh-*p53*(+). The Western blot results showed that the apoptosis-related proteins, *p53*, *Bax*, *PARP*, and cleaved *PARP*, were decreased in the group with *DINO*(–) + sh-*p53*(+). However, when *DINO* was present in the group with *DINO*(+) + sh-*p53*(+), it partially reversed the apoptosis-related proteins levels (*Figure 5A*). The IC50 was slightly increased in the group with *DINO*(–) + sh-*p53*(+) but partially reversed in the group with *DINO*(+) + sh-*p53*(+) (*Figure 5B*). A similar experiment yielded comparable results, as flow cytometry showed moderate enhancement of cell apoptosis in the LV-*DINO* + sh-*p53* group compared to the LV-NC + sh-*p53* group (*Figure 5C,5D*).

The Bax gene was regulated by the tumor suppressor p53 and was an important component in cell apoptosis

We generated *Bax* knockout (ko-*Bax*) cells using the CRISPR/Cas9 system. The CCK-8 assays showed that

the IC50 was significantly reduced after the cotransfection of LV-*DINO* and ko-*Bax* vectors (as compared to the LV-NC + ko-*Bax* group) (*Figure 5E*). Also, flow cytometry demonstrated a significant reduction in apoptosis in the LV-NC + ko-*Bax* group. However, in the group with cotransfection of LV-*DINO* + ko-*Bax*, this effect on apoptosis was reversed (*Figure 5F,5G*). These data suggest that the lncRNA *DINO* regulates chemotherapy-induced apoptosis via the *p53-Bax* axis.

LncRNA DINO enhanced DDP sensitivity in vivo

To further assess the effect of the lncRNA *DINO* on the sensitivity of NSCLC cells to DDP *in vivo*, A549R-LV-NC or A549R-LV-*DINO* cells were inoculated into the right flank of immunocompromised nude mice. After 7 days of tumor formation, the nude mice were intraperitoneally injected with DDP (2 mg/kg) or PBS, and the tumor volume was subsequently measured. After 21 days of recording, the A549R-LV-*DINO*-inoculated mice showed a significantly decreased tumor volume and weight compared with the A549R-LV-NC mice (*Figure 6A-6C*). H&E staining showed that the group with lncRNA *DINO* up-regulation had a higher degree of necrosis, while the LV-NC group exhibited almost no observable necrosis. IHC analysis showed that the lncRNA *DINO* up-regulation significantly increased the apoptosis-related protein, *Bax*, and decreased the anti-apoptotic protein, *Bcl-2* (*Figure 6D*). Together, these data suggested that lncRNA *DINO* overexpression sensitized NSCLC cells to DDP *in vivo*.

Discussion

At present, the main pathological type of lung cancer is NSCLC, which has the highest mortality rate among all malignant tumors (1); 57% of lung cancer patients have metastatic disease at the time of diagnosis, and their 5-year relative survival rate is less than 20% (26). Currently targeted therapy is recommended as first line treatment for patient with sensitive mutation. But all patients with mutation will be resistant to targeted therapy eventually. Then chemotherapy will be the treatment choice. Thus, the issue of DDP resistance will be problem for all patients, with or without sensitive mutation (27,28). Herein, we reported that the lncRNA *DINO* reduced DDP resistance via the *p53-Bax* axis through *p53* stability.

We first analyzed the relative expression of the lncRNA *DINO* in eight cell lines and found that compared with
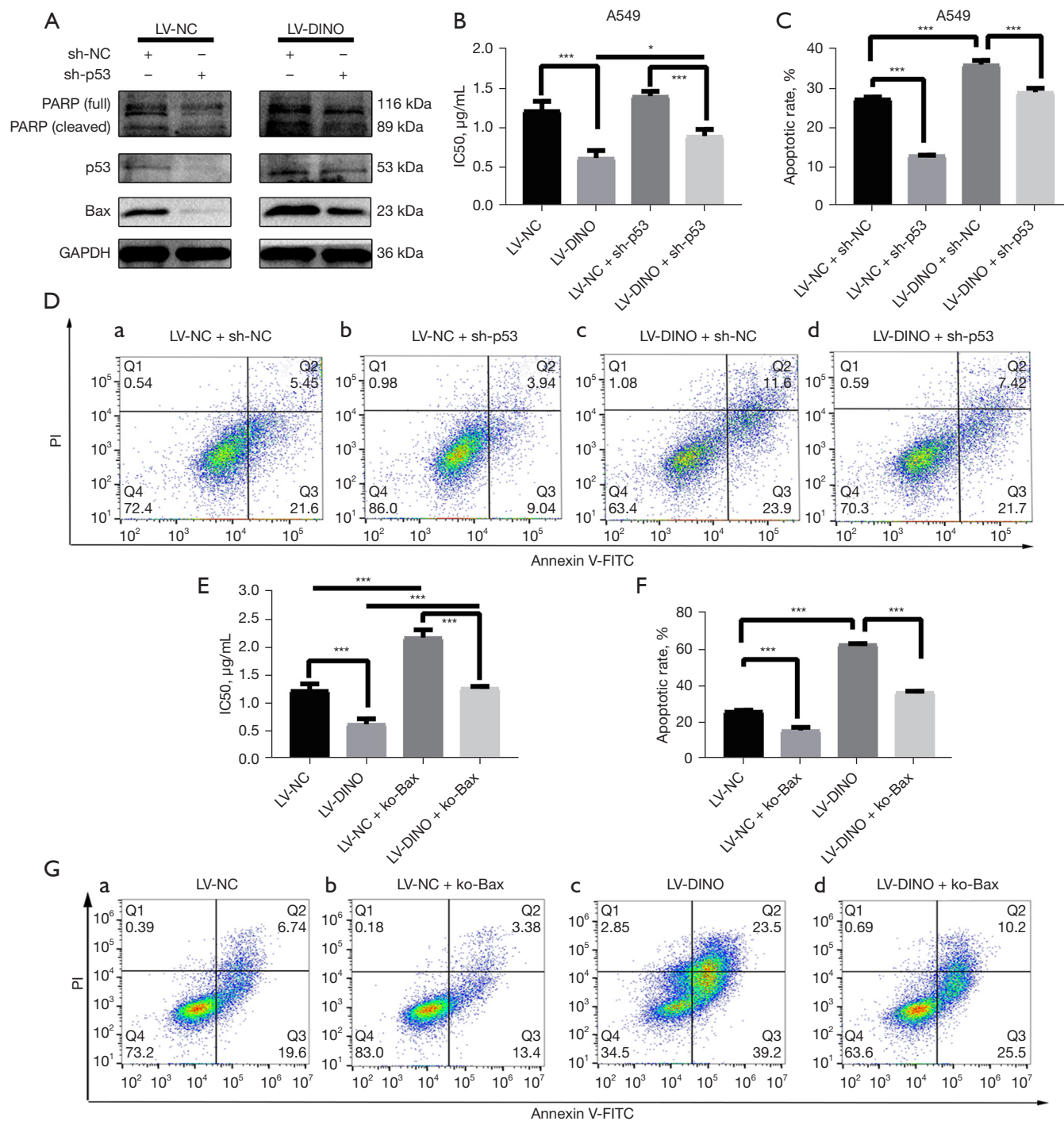
Figure 5 LncRNA *DINO* can partially reverse cisplatin resistance after silencing the *p53-Bax* axis. (A) Western blot was used to detect the changes of PARP, p53, and Bax protein expression in A549 cells co-transfected with LV-*DINO* and sh-*p53*. (B) The IC50 of cisplatin was measured by CCK-8 assays with A549 cells co-transfected with LV-*DINO* and sh-*p53*. (C) The statistical analysis of the total apoptosis rate to (D). (D) The cell apoptosis rate was determined by flow cytometry. (E) The IC50 of cisplatin was measured by CCK-8 assays with A549 cells co-transfected with LV-*DINO* and ko-*Bax*. (F) The statistical analysis of the total apoptosis rate to (G). (G) The cell apoptosis rate was determined by flow cytometry. *, P<0.05; ***, P<0.001. CCK-8, Cell Counting Kit-8; DINO, damage-induced non-coding; FITC, fluorescein isothiocyanate; GAPDH, glyceraldehyde 3-phosphate dehydrogenase; ko, knockout; lncRNA, long non-coding RNA; LV, lentivirus; NC, negative control; PARP, poly-(ADP-ribose) polymerase; PI, propidium iodide; sh, small hairpin.
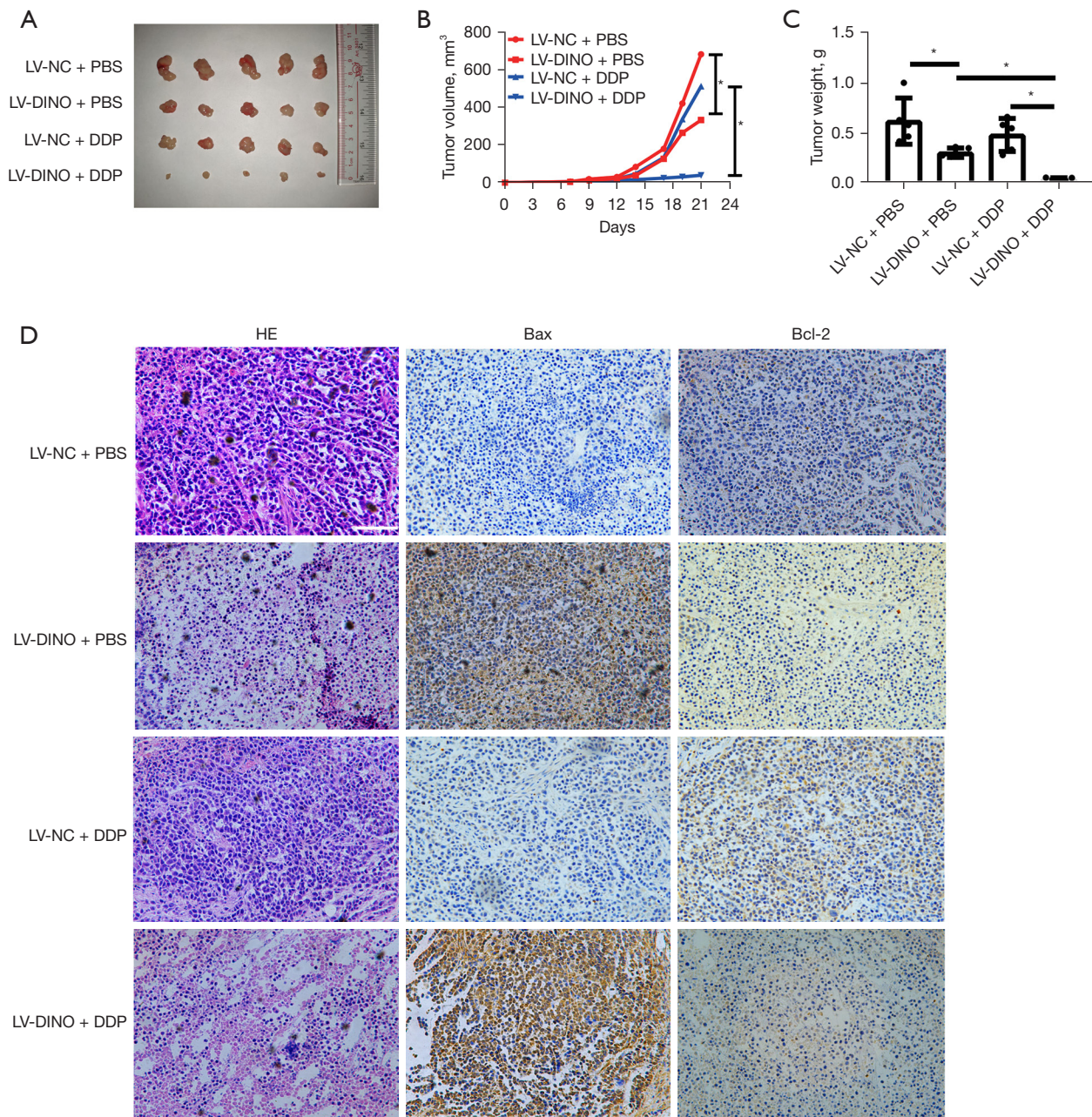
Figure 6 LncRNA *DINO* enhances DDP sensitivity *in vivo*. (A) Tumors that formed in a nude mice tumor model after injection of A549R-LV-NC or A549R-LV-*DINO* cells treated with DDP (2 mg/kg) or PBS, twice a week for 2 weeks. (B) Tumor volume was recorded every 3 days. (C) Tumor weight was recorded. (D) H&E and IHC analysis of Bax and Bcl-2 expressions in the derived tumor xenograft. Scale bar =100 μm. *, P<0.05; DDP, cisplatin; DINO, damage-induced non-coding; H&E, hematoxylin and eosin; IHC, immunohistochemistry; lncRNA, long non-coding RNA; LV, lentivirus; NC, negative control; PBS, phosphate-buffered saline.

normal lung epithelial HBE cells, the lung cancer cell lines showed significant down-regulation of the lncRNA *DINO*. A growing number of studies have noted that lncRNAs can be biomarkers; for example, prostate cancer associated 3

(*PCA3*) is the first biomarker approved by the U.S. Food and Drug Administration to predict prostate tumorigenesis (13). Follow-up reports have also found that a higher *PCA3* score (>60) is significantly related to identifying cancer from

an initial prostate biopsy (29). Furthermore, *AA174084* is expressed at low levels in gastric cancer, and the area under the receiver operating characteristic (ROC) curve is 0.848, suggesting that *AA174084* may be a biomarker for predicting gastric cancer (30). Increasing theoretical and experimental studies have shown that the down-regulation of the lncRNA *DINO* in lung mass biopsies may be a potential biomarker to assist pathologists in the diagnosis of early-stage lung cancer. In the future, biopsy specimens will be collected to test the relationship between lncRNA *DINO* and the clinical stage of lung cancer.

The lncRNA *DINO* is located at chr6:36,675,485–36,678,559 (GRCh38/hg38) and consists of 951 nucleotides in the upstream reverse transcription region of the *CDKN1A* gene. In the initial study, as human cells were damaged by doxorubicin, the expression of lncRNA *DINO* was upregulated, which promoted DNA damage repair pathways or cell apoptosis by binding to and stabilizing the *p53* protein (16). Subsequent research reports have pointed out that in acute liver injury, the lncRNA *DINO* is regulated by nuclear receptor subfamily 2 group E member 3 (*NR2E3*) to activate the *p53* pathway to reduce severe liver injuries (31). In cervical cancer, inducing lncRNA *DINO* expression can also increase the stability of the *p53* protein, thereby increasing the sensitization to chemotherapeutic agents and making cells more easily affected by metabolic pressure (32). Moreover, human papillomavirus 16 (HPV16) E7 can increase the expression level of *p53*, with the lncRNA *DINO* acting as the middle link between them (33). In HTR-8/SVneo human chorionic trophoblast cells, *DINO* has been shown to down-regulate the expression of matrix metallopeptidase 2 (*MMP2*) and inhibit the invasion and migration of these cells (34). In addition, *DINO* deficiency in mice has been linked to spontaneous tumorigenesis, with the tumor type being similar to that of human cancer, suggesting that *DINO* is an effective tumor suppressor molecule (35).

To identify the potential role of lncRNAs in DNA damage induced by DDP treatment, we investigated the functional relevance of the lncRNA *DINO* expression to DDP sensitivity in NSCLC. In the context of upregulated lncRNA *DINO* expression, increased apoptosis was observed during DDP treatment, and the *p53-Bax* axis was activated by the increase in *p53* stability. However, in the absence of lncRNA *DINO* expression, apoptosis was greatly reduced, and the *p53-bax* axis hardly responded. To further verify that the lncRNA *DINO* affects the DDP sensitivity of cells through the *p53-Bax* axis, a *p53* interference plasmid

was transfected; this treatment completely silenced the downstream genes of the *p53-Bax* axis and markedly reduced apoptosis. Consistent with these findings, in the virus group overexpressing the lncRNA *DINO*, the expression of the downstream genes of the *p53-Bax* axis was restored, and the drug resistance of the treated cells was reversed. Under normal circumstances, *Bax* needs to form a homologous complex to activate the mitochondria-dependent apoptosis program (36,37). However, recent reports have pointed out that *p53* can directly activate Bax in the cytoplasm by binding to structural regions, thereby triggering the corresponding cell death program (38). To explore the relationship between the lncRNA *DINO* and *p53-Bax* axis, a CRISPR-CAS9 system was designed to knock out the *Bax* gene as much as possible. Similarly, the CRISPR-CAS9 system that knocked out the *Bax* gene partially reversed DDP resistance after lentiviral overexpression of *DINO*.

Cell models are easily affected by the external environment in the culture medium, while the body is complex and relatively stable. For this reason, nude mice were used as a model for *in vivo* experiments to investigate the role of lncRNA *DINO* in the body. After subcutaneous tumor formation in the nude mice, the tumor volume in the lncRNA *DINO* overexpression group was relatively low. Evaluation of the dissected tumors also showed that the proapoptotic *Bax* protein was increased in the tumors of the lncRNA *DINO* overexpression group and that the antiapoptotic protein *Bcl-2* was decreased, and H&E staining showed increased necrosis. Before clinical application, safety and efficacy are the most important issues to be overcome with lncRNA, but by combining with nanomaterials, some lncRNA gene therapies have been applied in animal experiments and are expected to undergo subsequent clinical trials. For example, folate (FA)-modified liposomal (FA-LP) nanoparticles were loaded with the lncRNA metallothionein 1D, pseudogene (*MT1DP*) to regulate a protein kinase in NSCLC, which caused increased iron apoptosis (39). The lncRNA growth arrest specific 5 (*GAS5*) is significantly reduced in the serum of patients with type 2 diabetes mellitus (*T2DM*); therefore, to stabilize the level of *GAS5* in *T2DM*, Shi *et al.* used the small molecule NP-C86, which can bind to *GAS5* with high affinity and increase the levels of *GAS5* and glucose uptake in the adipocytes of diabetic patients (40).

Conclusions

The lncRNA *DINO* stabilizes *p53* to mediate the activation

J Thorac Dis 2023;15(4):2198-2212 | https://dx.doi.org/10.21037/jtd-23-465

2210

Liu et al. LncRNA *DINO* enhances cisplatin sensitivity

of the *p53-Bax* axis and regulate the sensitivity of LUAD to DDP. Together, our results suggest that research on the lncRNA *DINO* may provide a new understanding of the mechanisms of DDP sensitivity and help in the development of novel and effective strategies to treat NSCLC.

Footnote

Reporting Checklist: The authors have completed the ARRIVE reporting checklist. Available at https://jtd.amegroups.com/article/view/10.21037/jtd-23-465/rc

Data Sharing Statement: Available at https://jtd.amegroups.com/article/view/10.21037/jtd-23-465/dss

Peer Review File: Available at https://jtd.amegroups.com/article/view/10.21037/jtd-23-465/prf

Conflicts of Interest: All authors have completed the ICMJE uniform disclosure form (available at https://jtd.amegroups.com/article/view/10.21037/jtd-23-465/coif). The authors have no conflicts of interest to declare.

Ethical Statement: The authors are accountable for all aspects of the work in ensuring that questions related to the accuracy or integrity of any part of the work are appropriately investigated and resolved. Animal experiments were performed under a project license (No. 2018A0303130233) granted by institutional ethics board of Southern Medical University, in compliance with institutional guidelines for the care and use of animals.

Open Access Statement: This is an Open Access article distributed in accordance with the Creative Commons Attribution-NonCommercial-NoDerivs 4.0 International

References

1. Siegel RL, Miller KD, Wagle NS, et al. Cancer statistics, 2023. CA Cancer J Clin 2023;73:17-48.
2. Seguin L, Durandy M, Feral CC. Lung Adenocarcinoma Tumor Origin: A Guide for Personalized Medicine. Cancers (Basel) 2022;14:1759.
3. Ettinger DS, Wood DE, Aisner DL, et al. Non-Small Cell Lung Cancer, Version 3.2022, NCCN Clinical Practice Guidelines in Oncology. J Natl Compr Canc Netw 2022;20:497-530.
4. Maconachie R, Mercer T, Navani N, et al. Lung cancer: diagnosis and management: summary of updated NICE guidance. BMJ 2019;364:l1049.
5. Chen P, Liu Y, Wen Y, et al. Non-small cell lung cancer in China. Cancer Commun (Lond) 2022;42:937-70.
6. Guo WJ, Zhang YM, Zhang L, et al. Novel monofunctional platinum (II) complex Mono-Pt induces apoptosis-independent autophagic cell death in human ovarian carcinoma cells, distinct from cisplatin. Autophagy 2013;9:996-1008.
7. De Santis M, Bellmunt J, Mead G, et al. Randomized phase II/III trial assessing gemcitabine/carboplatin and methotrexate/carboplatin/vinblastine in patients with advanced urothelial cancer who are unfit for cisplatin-based chemotherapy: EORTC study 30986. J Clin Oncol 2012;30:191-9.
8. Lu J, Wang W, Liu H, et al. Cisplatin induces calcium ion accumulation and hearing loss by causing functional alterations in calcium channels and exocytosis. Am J Transl Res 2019;11:6877-89.
9. Jungwirth U, Xanthos DN, Gojo J, et al. Anticancer activity of methyl-substituted oxaliplatin analogs. Mol Pharmacol 2012;81:719-28.
10. Eptaminitaki GC, Stellas D, Bonavida B, et al. Long non-coding RNAs (lncRNAs) signaling in cancer chemoresistance: From prediction to druggability. Drug Resist Updat 2022;65:100866.
11. Li Y, Jiang T, Zhou W, et al. Pan-cancer characterization of immune-related lncRNAs identifies potential oncogenic biomarkers. Nat Commun 2020;11:1000.

12. Schmitt AM, Chang HY. Long Noncoding RNAs: At the Intersection of Cancer and Chromatin Biology. Cold Spring Harb Perspect Med 2017;7:a026492.

13. Flynn RA, Chang HY. Long noncoding RNAs in cell-fate programming and reprogramming. Cell Stem Cell 2014;14:752-61.

14. Liao W, Du J, Wang Z, et al. The role and mechanism of noncoding RNAs in regulation of metabolic reprogramming in hepatocellular carcinoma. Int J Cancer 2022;151:337-47.

15. She K, He S, Lu X, et al. LncRNA SNHG7 promotes non-small cell lung cancer progression and cisplatin resistance by inducing autophagic activity. J Thorac Dis 2023;15:155-67.

16. Schmitt AM, Garcia JT, Hung T, et al. An inducible long noncoding RNA amplifies DNA damage signaling. Nat Genet 2016;48:1370-6.

17. Huarte M. p53 partners with RNA in the DNA damage response. Nat Genet 2016;48:1298-9.

18. Kastenhuber ER, Lowe SW. Putting p53 in Context. Cell 2017;170:1062-78.

19. Fetoni AR, Paciello F, Troiani D. Cisplatin Chemotherapy and Cochlear Damage: Otoprotective and Chemosensitization Properties of Polyphenols. Antioxid Redox Signal 2022;36:1229-45.

20. Ren N, Chen L, Li B, et al. Purified Tea (Camellia sinensis (L.) Kuntze) Flower Saponins Induce the p53-Dependent Intrinsic Apoptosis of Cisplatin-Resistant Ovarian Cancer Cells. Int J Mol Sci 2020;21:4324.

21. Balakrishnan K, Burger JA, Quiroga MP, et al. Influence of bone marrow stromal microenvironment on forodesine-induced responses in CLL primary cells. Blood 2010;116:1083-91.

22. Han MK, Song EK, Guo Y, et al. SIRT1 regulates apoptosis and Nanog expression in mouse embryonic stem cells by controlling p53 subcellular localization. Cell Stem Cell 2008;2:241-51.

23. Gao Y, Ma H, Gao C, et al. Tumor-promoting properties of miR-8084 in breast cancer through enhancing proliferation, suppressing apoptosis and inducing epithelial-mesenchymal transition. J Transl Med 2018;16:38.

24. Wang W, Zhao M, Cui L, et al. Characterization of a novel HDAC/RXR/HtrA1 signaling axis as a novel target to overcome cisplatin resistance in human non-small cell lung cancer. Mol Cancer 2020;19:134.

25. Zhong YF, Cheng J, Liu Y, et al. DNA Nanostructures as Pt(IV) Prodrug Delivery Systems to Combat Chemoresistance. Small 2020;16:e2003646.

26. Wang DY, Hong Y, Chen YG, et al. PEST-containing nuclear protein regulates cell proliferation, migration, and invasion in lung adenocarcinoma. Oncogenesis 2019;8:22.

27. Poels KE, Schoenfeld AJ, Makhnin A, et al. Identification of optimal dosing schedules of dacomitinib and osimertinib for a phase I/II trial in advanced EGFR-mutant non-small cell lung cancer. Nat Commun 2021;12:3697.

28. Hui R, Garon EB, Goldman JW, et al. Pembrolizumab as first-line therapy for patients with PD-L1-positive advanced non-small cell lung cancer: a phase 1 trial. Ann Oncol 2017;28:874-81.

29. Sanda MG, Feng Z, Howard DH, et al. Association Between Combined TMPRSS2:ERG and PCA3 RNA Urinary Testing and Detection of Aggressive Prostate Cancer. JAMA Oncol 2017;3:1085-93.

30. Shao Y, Ye M, Jiang X, et al. Gastric juice long noncoding RNA used as a tumor marker for screening gastric cancer. Cancer 2014;120:3320-8.

31. Khanal T, Leung YK, Jiang W, et al. NR2E3 is a key component in p53 activation by regulating a long noncoding RNA DINO in acute liver injuries. FASEB J 2019;33:8335-48.

32. Sharma S, Munger K. Expression of the Long Noncoding RNA DINO in Human Papillomavirus-Positive Cervical Cancer Cells Reactivates the Dormant TP53 Tumor Suppressor through ATM/CHK2 Signaling. mBio 2020;11:e01190-20.

33. Sharma S, Munger K. KDM6A-Mediated Expression of the Long Noncoding RNA DINO Causes TP53 Tumor Suppressor Stabilization in Human Papillomavirus 16 E7-Expressing Cells. J Virol 2020;94:e02178-19.

34. Wu K, Liu Y, Zhang H, et al. DNA damage induced long non-coding RNA (DINO) down-regulates the expression of MMP2 and inhibits the invasion and migration of human chorionic trophoblast cells. Xi Bao Yu Fen Zi Mian Yi Xue Za Zhi 2022;38:736-42.

35. Marney CB, Anderson ES, Baum R, et al. A Unique Spectrum of Spontaneous Tumors in Dino Knockout Mice Identifies Tissue-Specific Requirements for Tumor Suppression. Cells 2022;11:1818.

36. Godefroy N, Bouleau S, Gruel G, et al. Transcriptional repression by p53 promotes a Bcl-2-insensitive and mitochondria-independent pathway of apoptosis. Nucleic Acids Res 2004;32:4480-90.

37. Huang K, O'Neill KL, Li J, et al. BH3-only proteins target BCL-xL/MCL-1, not BAX/BAK, to initiate apoptosis. Cell Res 2019;29:942-52.

J Thorac Dis 2023;15(4):2198-2212 | https://dx.doi.org/10.21037/jtd-23-465

2212

Liu et al. LncRNA *DINO* enhances cisplatin sensitivity

38. Follis AV, Llambi F, Merritt P, et al. Pin1-Induced Proline Isomerization in Cytosolic p53 Mediates BAX Activation and Apoptosis. Mol Cell 2015;59:677-84.
39. Gai C, Liu C, Wu X, et al. MT1DP loaded by folate-modified liposomes sensitizes erastin-induced ferroptosis via regulating miR-365a-3p/NRF2 axis in non-small cell lung cancer cells. Cell Death Dis 2020;11:751.
40. Shi Y, Parag S, Patel R, et al. Stabilization of lncRNA GAS5 by a Small Molecule and Its Implications in Diabetic Adipocytes. Cell Chem Biol 2019;26:319-330.e6.

(English Language Editor: A. Kassem)

Table S1 Interference sequences used in the study

Targets	Sequences
DINO siRNA-1	5'-AAUCAUUCUGGCCUCAAGAUU-3'
DINO siRNA-2	5'-GGUUUAUGGAGAUGACAUA-3'
Sh-*DINO*	5'-AACTGGUUUAUGGAGAUGACAUAAAUUCAAGAGAUAUGUCAUCUCCAUAAACCAUUUUUUC-3'
Sh-*p53*	5'-GACTCCAGTGGTAATCTAC-3'
Bax-sg	5'-caccGTCGGAAAAAGACCTCTCGGGgttt-3'

DINO, damage-induced non-coding; sg, single-guide; sh, small hairpin; siRNA, small interfering RNA.

Table S2 Sequences of the primers used in the study

Gene	Forward	Reverse
DINO	GGAGGCAAAAGTCCTGTGTT	GGGCTCAGA GAAGTCTGGTG
GAPDH	GTCGGAGTCAACGGATTTG	TGGGTGGAATCATATTGGAA
CDKN1A	TGTCCGTCAGAACCCATGC	AAAGTCGAAGTTCCATCGCTC
p53	GAGGTTGGCTCTGACTGTACC	TCCGTCCCAGTAGATTACCAC
Bax	CCCGAGAGGTCTTTTTCCGAG	CCAGCCCATGATGGTTCTGAT
GADD45A	GAGAGCAGAAGACCGAAAGGA	CAGTGATCGTGCGCTGACT
Fas	TCTGGTTCTTACGTCTGTTGC	CTGTGCAGTCCCTAGCTTTCC

DINO, damage-induced non-coding; GAPDH, glyceraldehyde 3-phosphate dehydrogenase.